

## ADSORPTION STUDIES AND FLUORIDE REMOVAL FROM AQUEOUS SOLUTIONS BY GRAPHENE OXIDE - ZINC OXIDE NANOCOMPOSITE

C. S. CHAKRA<sup>a\*</sup>, V. S. SAI KUMAR<sup>b</sup>, S. MADHURI<sup>a</sup>, P. ANUSHA<sup>a</sup>,  
T. R. KUMAR<sup>a</sup>, D. RAKESH<sup>a</sup>

<sup>a</sup>Centre for Nano Science and Technology, Institute of Science and Technology,  
Jawaharlal Nehru Technological University Hyderabad, Hyderabad 500085,  
Telangana, India

<sup>b</sup>Department of Physics, Guru Nanak Institute of Technology, Ibrahimpatnam,  
501506, Telangana, India

Drinking water offers several essential elements for the human beings; however the existence of a few dissolved elements other than acceptable concentration can cause danger to health of humans. In general the suspended elements in water have fluoride, but fluoride at very low concentrations or at very high concentrations may cause undesirable health effects. Hence it needs to be placed at acceptable levels. In the present study, we report synthesis and characterization of graphene oxide - zinc oxide nanocomposite and their usage for fluoride removal is discussed. The graphene oxide - zinc oxide nanocomposite adsorbent offers a synergy toward fluoride removal from contaminated drinking water. Thus prepared graphene oxide - zinc oxide nanocomposite and the effects of contact time for the removal of fluoride were evaluated. The Langmuir and Freundlich isotherms were utilized to explain adsorption equilibrium for fluoride removal by graphene oxide - zinc oxide nanocomposite. (k).

(Received December 2, 2018; Accepted March 8, 2019)

*Keywords:* Graphene-zinc oxide nanocomposite, Fluoride removal, Adsorption studies

### 1. Introduction

Groundwater remains the solitary preference in several under developed and developing countries such as India for the everyday requirements and requirements of people. On the other hand unfortunately, owing to over exploitation and weathering of rocks, there is leakage of minerals in the groundwater that generally causes in the liberation of extra dissolved species inside the groundwater. The existences of a few of the dissolved elements are essential for health; however, occurrence of them other than the acceptable concentrations could direct to health problems. The chemical constituents in the drinking water will show adverse impacts. Related to a few usual elements, fluoride may enter the body via food ingestion, inhalation, and water and shows impact on our health. Approximately 80% of fluoride penetrate inside the body is excreted mostly by urine [1]. Elevated fluoride levels in the drinking water have turn out to be a essential health vulnerability at present as it persuades severe impact on human health including dental and skeletal fluorosis. Depending on the concentration and duration of uninterrupted absorption, the absorption of high amounts of fluoride could lead to Alzheimer's disease, arthritis, osteoporosis, brittle bones, infertility, cancer, brain damage, stained teeth, impaired metabolism of carbohydrates, and impaired DNA synthesis, lipids, minerals, vitamins and proteins [2]. In all elements, fluorine is highly electronegative and highly reactive and it's not originated in its elemental state in nature but occurs as fluorides [3] and is dangerous to health of humans. Besides natural sources fluorides can also be obtained from industrial activity or mining in a few regions. According to the World Health Organization (WHO) guidelines, the higher limit of concentration of fluoride in drinking water is 1.5 mg/L [4]. The mainly utilized techniques for the defluorination

---

\* Corresponding author: shilpachakra.nano@jntuh.ac.in

of water are as follows, they are precipitation, adsorption, electro dialysis, nanofiltration and ion-exchange, [5-13] Fluoride precipitation with aluminium and calcium salts [14, 15] has been intensively employed to eradicate fluoride ions from industrial wastewaters.

Adsorption is marked as the major technologies intended for the removal of fluoride in the drinking water while compared to the available technologies for removal of fluoride based on flexibility, simplicity of design, initial cost, ease of operation, and maintenance [16]. The effectiveness of this method mostly relies on adsorbents. Latest notice of scientists has been dedicated to the study of low cost and friendly reagents, from this reason, in the past years, substantial awareness has been focused on the study of fluoride removal using synthetic, biomass, and natural materials such as activated alumina [17], fly ash [18], alum sludge [19], chitosan beads [20,21], red mud [22], zeolite [23], calcite [24], hydrated cement [25], and layered double hydroxides[26].

In this present paper, we report synthesis and characterization of graphene oxide - zinc oxide nanocomposite and their usage for fluoride removal is discussed. The graphene oxide - zinc oxide nanocomposite adsorbent offers a synergy toward removal of fluoride ions from contaminated drinking water. Thus prepared graphene oxide - zinc oxide nanocomposite and the effects of contact time for the removal of fluoride were assessed. The adsorption equilibrium were illustrated by the Langmuir and Freundlich isotherms.

## **2. Materials and methods**

### **2.1. Synthesis of graphene oxide (GO) nanoparticles**

Graphene oxide was synthesized from graphite by a modified Hummer's method. For this purpose, concentrated  $\text{H}_2\text{SO}_4$  (23 ml) is added to a mixture of graphite flakes (1 gm) and  $\text{NaNO}_3$  (0.5 gm). The mixture was placed at low temperature (ice bath) and then  $\text{KMnO}_4$  (3 gm) was mixed drop wise to the above mixture and the reaction temperature of below  $20^\circ\text{C}$  is maintained while adding  $\text{KMnO}_4$ . Further in the next step of this process, the reaction mixture is warmed to  $35^\circ\text{C}$  and magnetically stirred for 30 min by the addition of (46 ml) distilled water gradually, during oxidation process the color change is observed from dark purplish-green to dark brown, after that the solution is cooled again in a water bath for 10 min to stop the oxidation process and additional water (140 ml),  $\text{H}_2\text{O}_2$  (1 ml) was further added then the mixture's color changes to bright yellow color representing a high oxidation level of graphite. The solution is then filtered and washed quite a lot of times with water which results in thickening of the solution comprising of graphene oxide nanoparticles. The washing process involves centrifugation of sample at 5000 rpm for half an hour, thereby producing high purity graphene oxide nanoparticles.

### **2.2. Preparation of Phyllanthus Emblica extract**

Phyllanthus emblica extract is prepared from Phyllanthus emblica leaves (50 gm). The leaves are cut into small pieces and washed twice to remove dirt on it. After that leaves are soaked in 400 ml of distilled water in a beaker and then they are heated on a hot plate for 2hrs at  $100^\circ\text{C}$ . The extract is filtered and collected from this beaker after cooling it.

### **2.3. Preparation of graphene oxide - ZnO nanocomposite by hydrothermal method**

The graphene oxide (0.45 g) was added to 50 ml of deionized water and ultra-sonicated for half an hour. Later than the solution pH is set to 4 by alkaline KOH solution and 0.5 M of zinc nitrate hexahydrate is mixed in the same solution and further 25 ml of Phyllanthus emblica extract is added to the same solution, stirred for 15 minutes, then the solution of pH got rised to 11 by ammonia solution which leads to high  $\text{Zn}(\text{OH})_2$  rate of conversion in its solution. The mixture was stirred vigorously for half an hour and placed in glass bottle of 100 ml and closed tightly with teflon seal and subsequently the glass bottle is kept in hot air oven for 10 hours at a temperature of  $80^\circ\text{C}$ . Once achieving this process, sample is cooled down to normal room temperature. The acquired graphene oxide - ZnO nanocomposite is washed and centrifuged quite a few times with water comprehensively. As prepared graphene oxide - ZnO nanocomposite dried inside oven for one day at  $70^\circ\text{C}$  to obtain a powdered form of the sample.

### 3. Results and discussion

#### 3.1. X-ray diffraction

The graphene oxide - ZnO nanocomposites are synthesized using zinc nitrate and graphene oxide at low temperature hydrothermal method with Phyllanthus Emblica extract. The XRD pattern of as prepared graphene oxide - ZnO nanocomposites is as shown in Fig. 1.

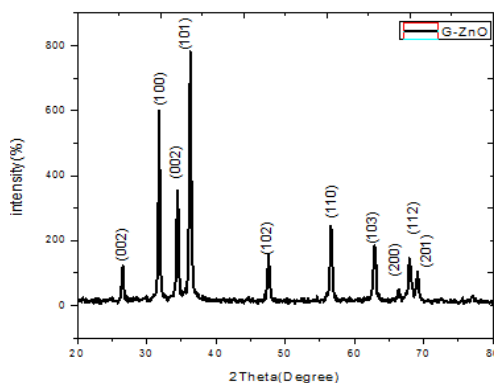


Fig. 1. XRD pattern of graphene oxide – ZnO nanocomposite.

The ZnO peaks are compared and indexed with standard JCPDS file no. 36 – 1451, which matches up to hexagonal wurtzite structure. The XRD result obviously specifies the formation of graphene oxide- ZnO nanocomposites with average crystalline size of 68.35nm. There is no peak which could be related to graphene, hence we can suggest that zinc oxide is mostly intercalated in graphene oxide. The characteristic peak for graphene oxide will be generally observed at  $11^{\circ}$ , but in general XRD can be scanned from  $20^{\circ} - 80^{\circ}$ . Therefore we didn't observed graphene oxide peak.

#### 3.2. Ultraviolet-visible spectroscopy

The absorbance spectrum of graphene oxide - ZnO nanocomposites is obtained by UV Visible spectrometer is as shown in Fig. 2. The observation of 375 nm peak confirmed the formation of ZnO in graphene – ZnO nanocomposite [27].

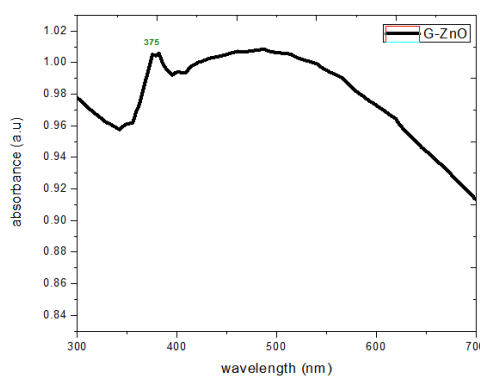


Fig. 2. UV absorbance spectrum of Graphene oxide –ZnO nanocomposite.

#### 3.3. Fourier transform infrared spectroscopy

The functional groups of graphene oxide - ZnO nanocomposite is analysed by FTIR spectrometer and the spectrum is as shown in Fig. 3. The observed peaks at  $3433$ ,  $1577$ ,  $1384$   $\text{cm}^{-1}$  are conveyed to graphene which correspond to OH group due to water moisture and tertiary C–OH vibration [27] correspondingly. The zinc oxide peak is observed at  $464$   $\text{cm}^{-1}$  which represents the

oxygen vacancy or oxygen deficiency defect complex in zinc oxide and it's a characteristic peak of  $E_2$  mode of ZnO hexagonal structure [27].

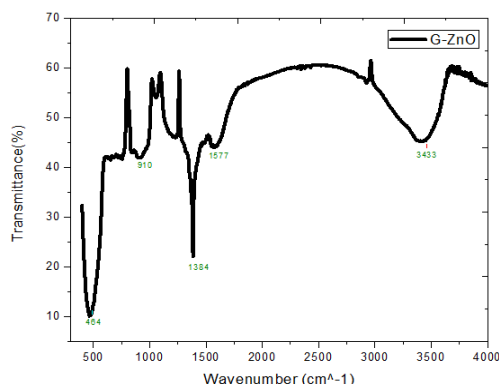


Fig. 3. FTIR spectrum of graphene Oxide - ZnO nanocomposite.

### 3.4. Field emission scanning electron microscopy

The surface morphology of the graphene oxide - ZnO nanocomposites obtained through low temperature hydrothermal technique are observed by field emission scanning electron microscopy (FESEM) and micrographs are as indicated in Fig. 4. The micrographs exposed that the ZnO nanoparticles are fixed perfectly on the surface of graphene oxide while little quantity of ZnO nanoparticles are intercalated among the graphene oxide sheets which outlines sandwich like structure [27].

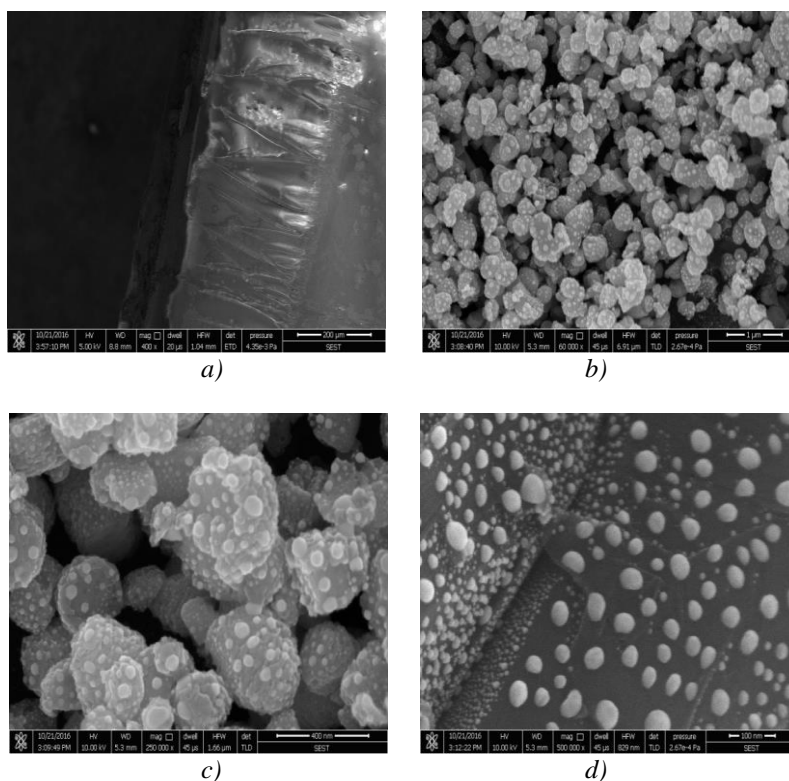


Fig. 4. FESEM image of Graphene oxide - ZnO nanocomposite (a) 20  $\mu\text{m}$  (b) 1  $\mu\text{m}$  (c) 400 nm and (d) 100 nm.

### 3.5. Transmission electron microscopy

The morphology of the graphene oxide - ZnO nanocomposites are viewed by transmission electron microscopy (TEM) and are as indicated in Fig. 5. The TEM image evidently signifying that the composite comprises of well distributed graphene oxide layers decorated by ZnO nanoparticles. These nanoparticles are uniformly dispersed on the graphene oxides which are clearly seen from the Fig. 5. Additionally, ZnO nanoparticles may not be viewed outside the graphene oxide layered material.

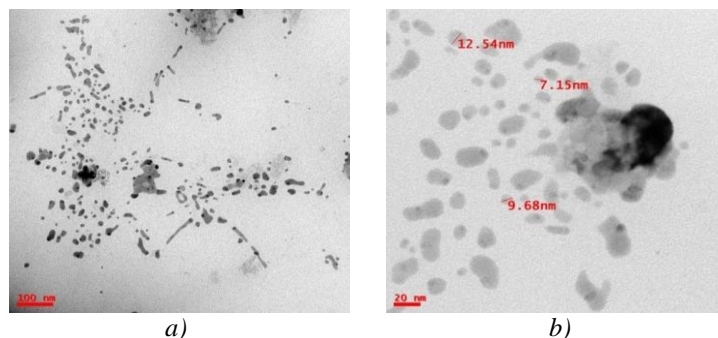


Fig. 5. TEM image of Graphene-ZnO nanocomposite (a) 100nm (b) 20nm.

The ZnO nanoparticles decorated over graphene oxide layer have uniform particle size of around 12 nm and are quasi spherical in shape. The contrast part in graphene oxide demonstrating the layer folds due to decoration of huge amount of ZnO nanoparticles on the graphene oxide. Fig. 6 indicates the selected area electron diffraction patterns of the graphene oxide - ZnO nanocomposites. The SAED patterns specified in Fig. 6 discloses that the obtained ZnO particles are having wurtzite structure with polycrystalline in nature [27].



Fig. 6. SAED pattern of Graphene-ZnO nanocomposite.

### 3.6. Dynamic light scattering analysis

Graphene oxide - ZnO nanocomposite synthesized are further characterized by by Dynamic Light Scattering for particle size distribution analysis. In the prepared graphene oxide - ZnO nanocomposite sample it is observed that particles have a wide size distribution, but most of them are well dispersed within a narrow range, as revealed in Fig 7. The average particle size of sample from the histogram is observed to be 54.2 nm.

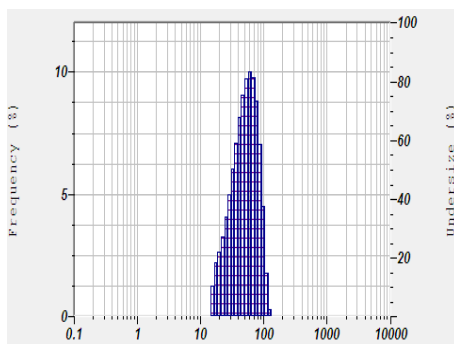


Fig. 7. Particle distribution in the dynamic light scattering of graphene oxide –ZnO nanocomposite.

### 3.7. Adsorption analysis

The adsorption analysis of graphene oxide – zinc oxide nanocomposite samples are analyzed for fluoride sample. Prior to UV light exposing, the solution is stirred for half an hour in dark to achieve absorption–desorption equilibrium between the sample and fluorine water. Fig. 8 indicates time dependent absorption of fluorine by Graphene–ZnO nanocomposite with 2 mg/L concentration.

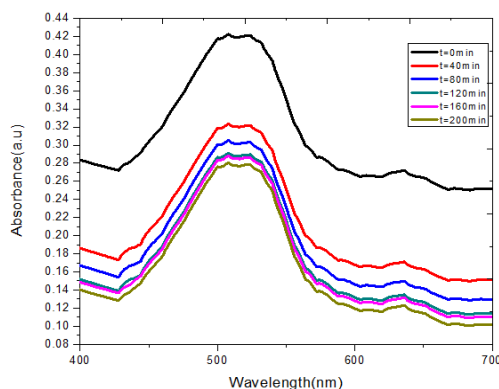


Fig. 8. Time dependent absorption of fluorine by Graphene–ZnO nanocomposite with 2 mg/L concentration.

Table 1. Absorbance of fluorine with time (2 mg/L) at 525 nm.

Time(min)	Absorbance(a.u.)
0	0.421
40	0.321
80	0.300
120	0.289
160	0.280
200	0.278
240	0.230

Here, we can observe that the absorption peak of fluorine is decreasing gradually with time. This experiment is conducted for 240 mins. By the end of the day the absorption peak was observed to be at 0.23(a.u).

Adsorption process can be illustrated by various models. Empirical models offer descriptions of adsorption data. Maximum adsorption capacity is an significant parameter to

characterize the performance of an adsorbent. Adsorption capacity is based on mass balance in the system adsorbent - adsorbate, considering that the adsorbate which is not found in the solution is retained by the adsorbent and is calculated with equation

A fluoride ion stock solution of 1000 mg/L is obtained by taking 221 mg of anhydrous sodium fluoride in volumetric flask by 100 mL distilled water. The fluoride adsorption capacity of adsorbent graphene oxide – zinc oxide nanocomposite is examined for different contact times. The defluoridation experiment is carried out by adding definite quantity of adsorbent with solution of sodium fluoride having a known fluoride concentration. The mixture is placed on a thermostatic shaker at a speed of 200 rpm at normal room temperature for a prearranged time to achieve the equilibrium. During the closing stages of equilibrium time, the solution is filtered and concentration of fluoride ions in water sample is measured by SPANDS process by UV/Vis spectrometer as per the practice of standard methods of inspection of waste water and water [28].

The fluoride removal efficiency (%) was calculated using equation (1):

$$Y (\%) = \frac{C_o - C_e}{C_o} \times 100 \quad (1)$$

Fluoride uptake ( $q_e$ ) was determined from eq. (2)

$$q_e = \frac{V}{m} (C_o - C_e) \quad (2)$$

where,  $C_o$  is the initial concentration (mg /L),  $C_e$  the concentration at equilibrium (gm/L),  $q_e$  the amount adsorbed at equilibrium (mg /g),  $m$  the adsorbent mass (gm) and  $V$  is the solution volume (L)

The analysis of the isotherm data by fitting to different isotherm models such as Langmuir and Freundlich is an important step to find the suitable model that can be used for design purposes. The Langmuir and Freundlich isotherms and their linearized forms are given in Table 2.

Table 2. Isotherms and their linear forms.

Isotherm	Form	Linear form	Plot	Ref
Langmuir	$q_e = \frac{q_m b C_e}{1 + K_a C_e}$	$C_e/q_e = 1/q_m C_e + 1/bq_m$	$C_e/q_e$ vs. $C_e$	[29]
Freundlich	$q_e = K_F C_e^{1/n_F}$	$\log(q_e) = \log(K_F) + 1/n_F \log(C_e)$	$\log(q_e)$ vs. $\log(C_e)$	[30]

where:  $C_e$  – equilibrium solute concentration, mg/l;  $q_e$  – amount of contaminant sorbed at equilibrium mg/g;  $K_F$  – Freundlich isotherm constant (mg/g) · (l/g) · 1/ $n_F$ ;  $n_F$  – Freundlich exponent;  $q_m$  – maximum sorption capacity, mg/g;  $b$ – Langmuir constant related to energy of adsorption, l/mg.

To appreciate how well correlates these mathematical model with experimental data obtained, experimental data fitting was performed with Langmuir and Freundlich isotherms equations. The results are presented in below figures.

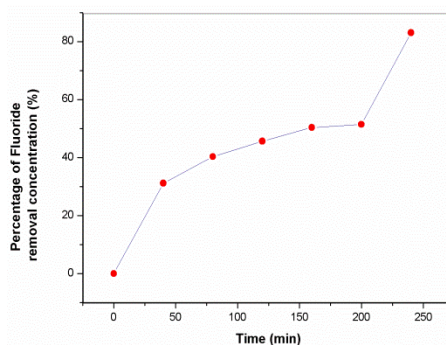


Fig. 9. Percentage of fluoride removal with contact time.

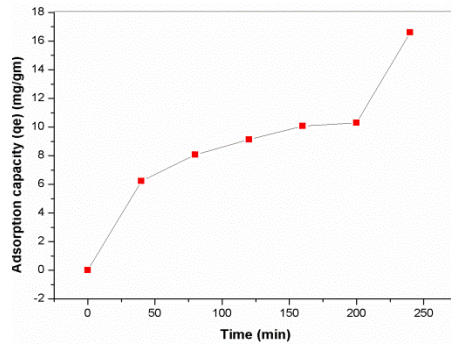


Fig. 10. Adsorption capacity of fluorine with contact time.

Adsorption capacity of fluorine Vs contact time was carried out by mixing 0.1 gm of Graphene oxide – zinc oxide nanocomposite adsorbent with 2 mg/L as initial fluoride concentration. Fig. 9 illustrates the removal of fluoride percentage versus contact time in the range of 0 –240 minutes at normal room temperature. The fluoride percentage values are escalating linearly up to 40 minutes and afterwards it remains nearly invariable signifying the accomplishment of adsorption equilibrium. Again suddenly at 200 minutes it showed the increase in value upto 240 minutes. Therefore 240 minutes was set as least contact time for the highest defluoridation of the sorbent.

Fig. 10 illustrates the adsorption capacity of fluoride adsorbed versus contact time in the range of 0 – 240 minutes at normal room temperature. The Graphene oxide – zinc oxide nanocomposite witnessed a greatest amount of fluoride adsorbed per gm of adsorbent ( $q_e$ ) was observed to be 16.608 mg/gm. This abrupt increase in the removal of fluoride point outs that the fluoride adsorption perhaps occur due to the diffusion intriguing position inside the pores on the adsorbent surface. The fluoride ions removal from water rises with increase in agitation time to a little degree.

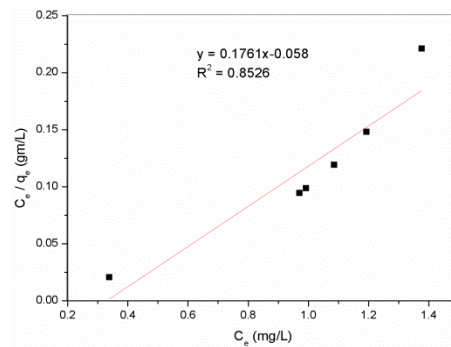


Fig. 11. Fluoride adsorption by Langmuir isotherm.

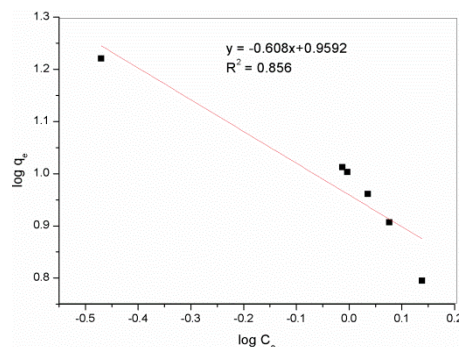


Fig. 12. Fluoride adsorption by Freundlich isotherm.

Table 3. Values for  $q_m, b, n_f$  and  $k_f$ .

<b>Langmuir isotherm</b>	From Slope $q_m = 5.6785$ mg/g	From intercept $b = 3.0362$ l/g
<b>Freundlich isotherm</b>	From Slope $n_f = 1.6447$	From intercept $k_f = 2.6096$ mg/g

Figs. 11 and 12 illustrates fluoride adsorption by Langmuir and Freundlich isotherms. Table 3 represents the values from the Langmuir and Freundlich isotherms. It is indicated in Table 3 that the magnitude of the Langmuir constant 'b' is observed to 3.0362 l/g. The values of  $q_m$  acquired from Langmuir model is 5.678 mg/g. The fitting of the Freundlich model to the adsorption isotherm implies that the magnitude of the Freundlich exponential constant,  $n_f$  has a value of 1.6447 and the Freundlich isotherm constant  $k_f$  has a value of 2.6096 mg/g. The elimination of fluoride ions from water is successful by graphene oxide / zinc oxide nanocomposite prepared by low temperature hydrothermal route.

#### 4. Conclusions

Graphene oxide / zinc oxide nanocomposite material is successfully prepared via low temperature hydrothermal method. The adsorption studies were performed using fluorine water. The graphene oxide /ZnO nanocomposites confirmed higher adsorption than from this results. The adsorption capacity of graphene oxide /ZnO nanocomposites for fluoride was 16.608 mg/g. The adsorption process equation was fitted well with both Langmuir and Freundlich isotherm models. 83 % of fluoride removal concentration is observed for a fluoride water of 2 mg /l. Hence graphene oxide / zinc oxide nanocomposite can be effectively used as adsorbent for removal of fluoride ions from drinking water.

#### References

- [1] H. Huang, K. Schwab, J. G. Jacangelo, Environ. Sci. Technol. **43**, 3011 (2009).
- [2] S. Ayoob, A. K. Gupta, Crit. Rev. Environ. Sci. Technol. **36**, 433 (2006).
- [3] A. A. M. Daifullah, S. M. Yakout, S. A. Elreefy, J. Hazard. Mater. **147**, 633 (2007).
- [4] WHO, Guidelines for Drinking Water Quality, 45, World Health Organization, Geneva, 1993.
- [5] A. M. Raichur, M. J. Basu, Sep. Purif. Technol. **24**, 121 (2001).
- [6] A. Tor, N. Danaoglu, G. Arslan, Y. Cengeloglu, J. Hazard. Mater. **164**, 271 (2009).
- [7] A. Tor, Desalination **201**, 267 (2006).
- [8] G. Singh, B. Kumar, P. K. Sen, J. Majumdar, Water Environ. Res. **7**, 36 (1999).
- [9] E. J. Rcardon, Y. Wang, Environ. Sci. Technol. **34**, 3247 (2000).
- [10] R. Simons, Desalination **89**, 1993, 325 (1993).
- [11] A. Tor, J. Hazard. Mater. **141**, 814 (2007).
- [12] M. Hichour, F. Persin, J. Sandeaux, J. Molenat, C. Gavach, Rev. Sci. Eau **12**, 671 (1999).
- [13] E. Ergun, A. Tor, Y. Cengeloglu, I. Kocak, Sep. Purif. Technol. **64**, 147 (2008).
- [14] S. Saha, Water Res. **27**, 1347 (1993).
- [15] M. Hichour, F. Persin, J. Sandeaux, C. Gavach, Sep. Purif. Technol. **18**, 1 (2000).
- [16] V. K. Gupta, I. Ali, V. K. Saini, Water Res. **41**, 3307 (2007).
- [17] S. Ayoob, A. K. Gupta, P. B. Bhakat, V. T. Bhat, J. Chem. Eng. **140**, 6 (2008).
- [18] A. K. Chaturvedi, K. P. Yadava, K. C. Pathak, V. N. Singh, Air Soil Pollut. **49**, 51 (1990).
- [19] M. G. Sujana, R. S. Thakur, S. B. Rao, Colloid Interface Sci. **275**, 355 (1998).
- [20] N. Viswanathan, C. S. Sundaram, S. Meenakshi, J. Hazard. Mater. **161**, 423 (2009).
- [21] N. Viswanathan, S. Meenakshi, J. Colloid Interface Sci. **322**, 375 (2008).
- [22] A. Tor, N. Danaoglu, G. Arslan, Y. Cengeloglu, J. Hazard. Mater. **164**, 271 (2009).
- [23] M. S. Onyango, Y. Kojima, O. Aoyi, E. C. Bernardo, H. Matsuda, J. Colloid Interface Sci.

- 279**, 341 (2004).
- [24] M. Yang, T. Hashimoto, N. Hoshi, H. Myoga, *Water. Res.* **33**, 3395 (1999).
- [25] N. I. Chubar, V. F. Samanidou, V. S. Kouts, G. G. Gallios, V. A. Kanibolotsky, V. V. Strelko, I. Z. Zhuravlev, *J. Colloid Interface Sci.* **291**, 67 (2005).
- [26] H.T. Wang, J. Chen, Y. F. Cai, J. F. Ji, L. W. Liu, H. H. Teng, *Appl. Clay Sci.* **35**, 59 (2007).
- [27] Balasubramaniam Saravanakumar, *Materials Research Bulletin* 0025-5408.
- [28] American Public Health Association, *Standard Methods for Examination of water and waste water* Washington DC, 2005.
- [29] S. Gotovac, H. Honda, Y. Hattori, K. Takahashi, H. Kanoh, K. Kaneko, *Nano Lett.* **7**, 583007)
- [30] K. V. Kumar, S. J. Sivanesan, *J. Hazard. Mat.* **126**, 198 (2005).